Two-particle spectra of heavy-fermion systems

P. Valášek, W. von der Linden, and V. Dose
Max-Planck-Institut für Plasmaphysik, Euratom Association, 85748 Garching bei München, Germany
(Received 24 October 1994)

Appearance-potential spectra of heavy-fermion systems are presented and analyzed in the frame of the Gunnarsson-Schönhammer approach for the Anderson-impurity model. This procedure has been used successfully to describe a wide variety of one-particle spectroscopies of $4f$ systems. Here we present a generalization of the Gunnarsson-Schönhammer approach for two-particle response functions, measured in appearance-potential spectroscopy. Calculations and experiments are presented for $CeNi_5$ and $CePd_3$. It appears that the first term in the $1/N$ expansion already gives strikingly good agreement with the experimental data and the Gunnarsson-Schönhammer approach describes two-particle response functions as reliably as those of one-particle spectra.

I. INTRODUCTION

In appearance-potential spectroscopy (APS) an incoming electron excites a core electron and both are scattered into unoccupied conduction band states. It therefore measures the unoccupied part of the two-particle density of states and can be considered as inverse Auger spectroscopy. Due to the small spatial extent of the core orbitals, APS is a local and element-specific probe and can be used for the chemical and magnetic characterization of surfaces and to study correlation effects.[1–3]

Routinely, APS spectra are described by self-convolution of the unoccupied part of the one-particle density of states.[4] This approximation is justified in spin-integrated spectra if matrix element effects are small and if the two additional electrons can be considered as independent quasiparticles. Cini and Sawatzky pointed out in the framework of the Hubbard model that the latter assumption can only be justified if the bandwidth is large compared to the Coulomb interaction.[5,6] Their analysis for an initially empty conduction band revealed a strong dependence of the resulting spectra on the interaction strength leading to either bandlike or atomic structures. A more thorough discussion of the importance of correlation effects for transition metals has been given by Nolting *et al.*[7–9] in the framework of a multiband Hubbard-type model. On the other hand, ignoring correlation effects, the band regime of APS spectra of many transition metals can be described satisfactorily by self-convolution of the density of states if matrix element effects are taken into account on a semiempirical level.[2] The situation is unambiguous, however, for heavy-fermion systems which belong to the realm of strong correlations indeed. For these materials, correlation effects become dominant in the APS process.

The Gunnarson-Schönhammer approach to the Anderson-impurity model has successfully described a wide variety of results of one-particle spectroscopies on $4f$ systems.[10] We shall show that APS spectra for heavy-fermion systems can be interpreted with similar success on this basis.

II. THEORY OF APS

We describe the heavy-fermion Ce compounds by the Anderson-impurity model (AIM), which contains all relevant terms for the physics of appearance potential spectroscopy. The AIM is used in the f-state representation and core hole terms are included as described in Ref. 11,

$$H^{\mathrm{AIM}} = \sum_{\nu}^{N_f} \int d\epsilon \epsilon \psi^{\dagger}_{\epsilon,\nu}\psi_{\epsilon,\nu} + \epsilon_f \sum_{\nu}^{N_f} \psi^{\dagger}_{\nu}\psi_{\nu} + \sum_{\nu}^{N_f} \int d\epsilon \left[V(\epsilon)\psi^{\dagger}_{\nu}\psi_{\epsilon,\nu} + \mathrm{H.c.}\right] + U \sum_{\nu,\mu}^{N_f} n_{\nu}n_{\mu} - U_{fc}(1-n_c)\sum_{\nu}^{N_f} n_{\nu} + \epsilon_c n_c \,. \quad (1)$$

Those parts of the original Hamiltonian, which have no influence on the $4f$ subsystem due to the different angular character, are discarded. The contributions to the Hamiltonian, as sketched in Fig. 1, are (a) the hopping term of conduction band electrons $(5d, 6s, 6p)$ [the respec-

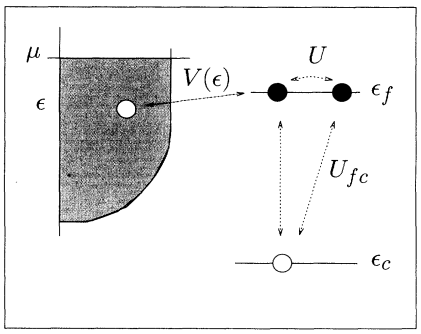

FIG. 1. Sketch of the physical processes covered by the AIM. The conduction band is filled up to chemical potential μ. Electrons in the f level at energy ϵ_f are scattered by the local Coulomb repulsion U, the core hole interaction U_{fc}, and the hybridization $V(\epsilon)$. The energy of the core level is ϵ_c.

tive creation (annihilation) operators are represented in a $4f$ orbital adapted basis; details are given in Ref. 11]; (b) the local potential for $4f$ electrons, which are created and annihilated by $\psi_\nu^\dagger$ and ψ_ν, respectively (the N_f degenerate $4f$ states are labeled by a combined orbital-spin index ν); (c) the hybridization of conduction and $4f$ electrons with the strength $V(\epsilon)$, which is assumed independent of ν; (d) the Hubbard interaction of $4f$ electrons with the interaction strength U; (e) the correction of the potential of the $4f$ electrons due to the presence of core holes;[12,13] and (f) the local potential of core electrons. The overlap between $4f$ states on nearest-neighbor sites is neglected because of the small spatial extent of the $4f$ orbitals. The model parameters U, U_{fc}, ϵ_f have been derived earlier by fitting calculated one-particle spectra such as x-ray photoemission spectroscopy, x-ray absorption spectroscopy (XAS), photoemission spectroscopy, and bremsstrahlung isochromat spectroscopy to experimental data.[10,14,15] The energy-dependent hybridization $V(\epsilon)$ is approximated by the standard expression

$$V^2(\epsilon_i) = \frac{\Delta}{N_f \pi^2 B}\sqrt{B^2 - (\epsilon_i - B_0)^2}. \tag{2}$$

$2B$ is the conduction band width, B_0 a fit parameter for the elliptical form, and Δ the hybridization strength.

To begin with, we want to discuss qualitatively why the self-convolution breaks down in the case of strongly correlated electrons. The APS intensities are proportional to the probability for putting two electrons into the unoccupied states under consideration. Energy conservation demands that the sum of both electronic energies is fixed to a value ω

$$\mathcal{I}^{\mathrm{APS}}(\omega) \propto \iint \mathcal{P}(E_1 = \omega_1 \wedge E_2 = \omega_2) \times \delta(\omega_1 + \omega_2 - \omega) d\omega_1 d\omega_2 \ .$$

$\mathcal{P}(E_1 = \omega_1 \wedge \mathrm{E}_2 = \omega_2)$ stands for the joint probability for the two electrons having energy ω_1 and ω_2, respectively. The δ function guarantees energy conservation. The joint probability may be rewritten in terms of $\mathcal{P}(E_1 = \omega_1)$ and the conditional probability $\mathcal{P}(E_2 = \omega - \omega_1 | E_1 = \omega_1)$

$$\mathcal{I}^{\mathrm{APS}}(\omega) \propto \int \mathcal{P}(E_1 = \omega_1) \times \mathcal{P}(E_2 = \omega - \omega_1 | E_1 = \omega_1) d\omega_1 \ .$$

If the probability of putting the second electron into the system is independent of the presence of the first one, we end up with a self-convolution of the unoccupied density of states (DOS) $\tilde{\rho}$

$$\mathcal{I}^{\mathrm{APS}}_{\mathrm{uncorr}}(\omega) \propto \int \mathcal{P}(E_1 = \omega_1)\mathcal{P}(E_2 = \omega - \omega_1) d\omega_1 \propto \int \tilde{\rho}(\omega_1)\tilde{\rho}(\omega - \omega_1) d\omega_1 \ ,$$

which works well for the spin-integrated APS spectra of Fe or Cu with broad unoccupied DOS.[1] The situation is different in the APS process of Ce compounds measuring the $\mathbf{M}_V$ $(3d_{5/2} \rightarrow 4f)$ and $\mathbf{M}_{IV}$ $(3d_{3/2} \rightarrow 4f)$ transitions. Both electrons occupy the same f orbital and therefore experience a strong mutual correlation U and a pronounced interaction with the core hole U_{fc}. In this case, due to the local nature of the APS process, there is a marked difference between the probability for putting the first electron into the system and the conditional probability for adding a second electron, given the presence of the first one. We will see below that in the heavy-fermion systems a self-convolution leads to unphysical results.

To determine the APS intensities, we invoke Fermi's golden rule. The APS process leading from an initial state $|i\rangle$ to a final state $|f\rangle$ is depicted in Fig. 2. By $|\Psi_0\rangle$ we denote the exact many-body ground state of the N-particle system. The initial state $|i\rangle = a^\dagger_{k,\sigma}|\Psi_0\rangle$ describes the system with an incident high-energy electron. Due to the local nature of the APS process the relevant final states in the energy range, detected by the APS process under consideration, are $|f\rangle = \psi^\dagger_{i,\nu}\psi^\dagger_{i,\mu}\psi_{c_i}|\Psi_0\rangle$. Fermi's golden rule yields

$$\begin{aligned}
\mathcal{I}^{\mathrm{APS}}(\omega) &\simeq \sum_f \left|\langle f|\tilde{H}|i\rangle\right|^2 \delta(\underbrace{\omega + E_0}_{E_i} - E_f) \\
&\simeq \sum_f \left|\langle f|\tilde{H}a^\dagger_{k,\sigma}|\Psi_0\rangle\right|^2 \mathrm{Im}\left(\frac{1}{\omega + E_0 - E_f + i\delta}\right) \\
&\simeq \mathrm{Im}\sum_f \left\langle \Psi_0 \middle| a_{k,\sigma'}\tilde{H}^\dagger \frac{1}{\omega + E_0 - H + i\delta} \middle| f \right\rangle \langle f| \underbrace{\tilde{H}a^\dagger_{k,\sigma}}_{\mathcal{T}^\dagger} |\Psi_0\rangle \\
&\simeq \mathrm{Im}\left\langle \Psi_0 \middle| \mathcal{T}\frac{1}{\omega + E_0 - H + i\delta}\mathcal{T}^\dagger \middle| \Psi_0 \right\rangle \\
&\simeq \mathrm{Im}\,\mathcal{G}(\omega).
\end{aligned} \tag{3}$$

We restrict the Coulomb interaction $\tilde{H}$ such that it only scatters into the experimentally relevant final states. The restricted operator is called $\mathcal{T}^\dagger$. This allows us to employ the closure relation $\sum_f |f\rangle\langle f| = \mathbf{1}$. The operator $\mathcal{T}^\dagger$ describes the local APS process and reads in general

$$\mathcal{T}^\dagger = \sum_{\substack{i \\ \nu,\mu}} V_{i,\nu,\mu}\ \psi^\dagger_{i,\nu}\psi^\dagger_{i,\mu}\psi_{c_i} \ .$$

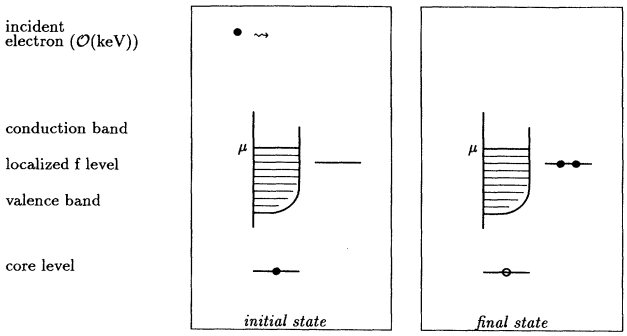

FIG. 2. Initial state and final state of the APS process.

A core electron is removed and two f electrons are created. V describes the Coulomb interaction between the relevant states. Notice that no optical selection rules apply in the APS experiment.

Next we follow the ideas of Gunnarsson and Schönhammer[10,11,14,16] and ignore the dynamics of the core hole, which reduces the problem to computing the two-particle Green's function for $4f$ electrons in the presence of a core hole. It is to be expected that the core hole dynamics does not change the energetic position of the peaks. It merely leads to an additional lifetime broading. This conjecture is corroborated by the difference in experimental APS data for Ni obtained by detecting subsequent Auger or x-ray processes.[17] The influence of core hole dynamics on the APS intensities for transition metals has been studied recently.[9] To evaluate Fermi's golden rule we need the many-body ground state $|\Psi_0\rangle$ with corresponding energy E_0. Furthermore, we need the excited APS states $|f\rangle = \psi^\dagger_{i,\nu}\psi^\dagger_{i,\mu}\psi_{c_i}|\Psi_0\rangle$ to calculate the matrix elements $\langle f'|(\omega + E_0 - H + i\delta)^{-1}|f\rangle$ entering the Green's function $\mathcal{G}(\omega)$ and $\mathcal{I}^{\mathrm{APS}}(\omega)$, respectively. Here we will use an approach similar to the one introduced by Gunnarsson and Schönhammer[10] (GS) to describe one-particle spectra. To determine dynamic properties of the Anderson model a $\frac{1}{N_f}$ expansion is used[18,19] to define a restricted set of basis functions for a variational calculation. The ground state is calculated using a trial wave function representing the first-order terms of the $1/N_f$ expansion (Fig. 3)

$$|\Psi_0\rangle = \mathcal{A}\left[1 + \sum_\nu \int d\epsilon \mathcal{B}(\epsilon)\psi^\dagger_\nu \psi_{\epsilon,\nu}\right]|f^0\rangle \ .$$

Upon minimizing the energy, the ground state energy

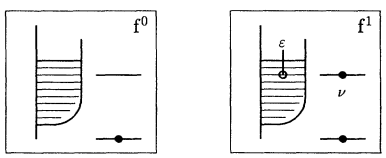

FIG. 3. Basis states for the ground state.

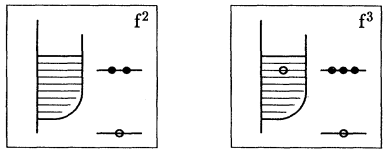

FIG. 4. Basis states for the final state.

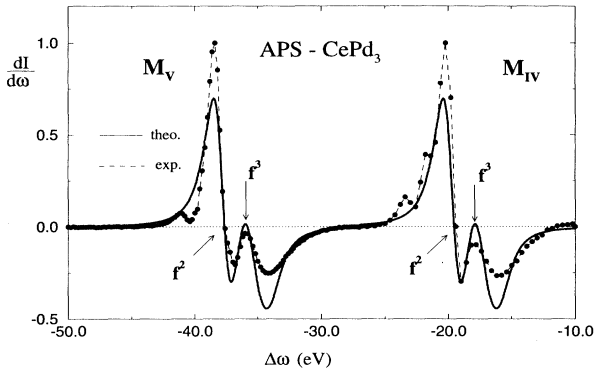

FIG. 5. Theoretical result (solid line) for the first derivative of the APS intensity (arb. units) for $CePd_3$ compared to normalized experimental data (dashed line). The energy scale is relative to the incident electron energy.

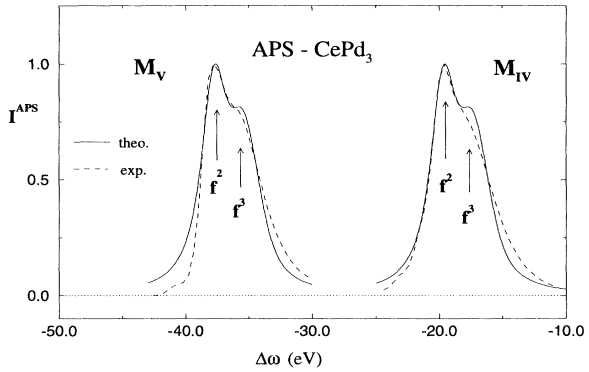

FIG. 6. Separately integrated and normalized spectra of Fig. 5 for $CePd_3$ (arb. units). A linear background was subtracted from the experimental data.

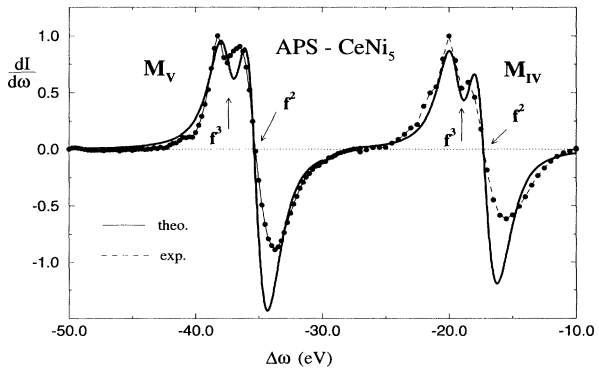

FIG. 7. Theoretical result (solid line) of the first derivative of the APS intensity (arb. units) for $CeNi_5$ compared to normalized experimental data (dashed line). The energy scale is relative to the incident electron energy.

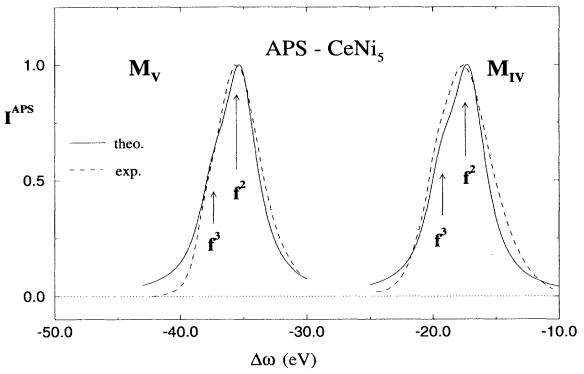

FIG. 8. Separately integrated and normalized spectra of Fig. 7 for $CeNi_5$ (arb. units). A linear background was subtracted from the experimental data.

E_0 and the coefficients $\mathcal{A}$ and $\mathcal{B}(\epsilon)$ are determined. We introduce the abbreviation

$$|\Psi_0\rangle = c_0 |f^0\rangle + c_1 |f^1\rangle .$$

The subspace of dominant excited states is obtained upon applying $\mathcal{T}^\dagger$ to the ground state, leading to states which represent the first-order final states of the APS process (Fig. 4). Note that site indices have been dropped since there is only one $4f$ site in the AIM. Put differently, we do not allow the $4f$ electrons to propagate during the measurement

$$\psi_\nu^\dagger \psi_\mu^\dagger \psi_c |\Psi_0\rangle = \mathcal{A} \Bigg[\underbrace{\psi_\nu^\dagger \psi_\mu^\dagger}_{|\nu\mu\rangle} + \int d\epsilon \underbrace{\sum_\lambda \mathcal{B}_\lambda(\epsilon) \psi_\lambda^\dagger \psi_{\epsilon,\lambda} \psi_\nu^\dagger \psi_\mu^\dagger}_{|\nu\mu\epsilon\rangle} \Bigg] \psi_c |f^0\rangle$$

$$|f\rangle \propto \tilde{c_0} |f^2\rangle + \tilde{c_1} |f^3\rangle .$$

The computation of the matrix elements of $(\omega + E_0 - H + i\delta)^{-1}$ and H are restricted to the subspace, spanned by $|\nu, \mu\rangle$ and $|\nu, \mu, \epsilon\rangle$. It should be mentioned that the width of the APS intensities within the GS approach is entirely governed by the parameter δ.

III. RESULTS

Experimental and theoretical APS intensities for $CePd_3$ and $CeNi_5$ will be presented. Appearance potential spectra are usually measured with lock-in techniques. This allows one to separate the strong continuous bremsstrahlung background from the signal due to core hole excitation. The experiment provides therefore the first derivative of the calculated excitation spectra. The results are depicted in Figs. 5 and 6 for $CePd_3$ and in Figs. 7 and 8 for $CeNi_5$. Peaks in the integrated experimental spectra Figs. 6 and 8, i.e., zeros in the differential spectra of Figs. 5 and 7, correspond to integer $4f$ occupancies in the excited states, as indicated in the figures. In both examples the peak positions are in strikingly good agreement with the experimental data. The parameters used in our calculation are given in Table I. They are the same as previously used for the one-particle spectra. Only the core level energy ϵ_c and the hybridization strengh Δ had to be readjusted. A broadening accounting for the resolution of the present experiment and the core hole lifetime was finally included. In spite of the strong Coulomb repulsion $U = 6.8$ eV the f^3 peaks of $CePd_3$ appear close to the f^2 peaks, due to the core hole interaction $\left(\mathbf{M}_V : \omega_{f^2 \leftrightarrow f^3} = 1.7 \pm 0.1 \text{ eV}\right)$. There are slight additional structures in the experimental spectra below the f^2 peaks. They cannot be explained by improving the basis set in the GS approach, as all structures resulting from excited states involving more than three electrons appear above the f^3 peaks. Similar structures have been observed earlier in core electron-energy-loss spectroscopy data and have been attributed to final state multiplets,[20] which are not included in the present treatment. The importance of the core hole interaction becomes particularly apparent in the case of $CeNi_5$ (Fig. 7). Here the f^3 peaks, despite the stronger Coulomb repulsion, are shifted to energies below the f^2 states $\left(\mathbf{M}_V : \omega_{f^2 \leftrightarrow f^3} = 2.3 \pm 0.2 \text{ eV}\right)$. This feature is reproduced by the theoretical result. Finally, we should mention that multiple final states in APS do not indicate mixed valency in the initial state. A one-particle approximation for the APS intensity is obtained by a self-convolution of XAS spectra. But calculations, for example, for XAS spectra of $CePd_3$ show a splitting between the f^1 and f^2 peaks of $\simeq 5.3$ eV. This would lead to a splitting of the f^2 and f^3 peaks by the same value of 5.3 eV, as compared to 1.7 eV observed in the experiment and found in our calculation. In addition there

TABLE I. The model parameters used in Eqs. (1)–(3) fitted for the different transitions. For all spectra we used the f degeneracy $N_f = 14$, the bandwidth $B = 2.005$ eV, and the hybridization parameter $B_0 = -1.995$ eV.

Parameter (eV)	$\mathbf{M}_V$:$CePd_3$	$\mathbf{M}_{IV}$:$CePd_3$	$\mathbf{M}_V$:$CeNi_5$	$\mathbf{M}_{IV}$:$CeNi_5$
Δ	0.28	0.28	0.18	0.19
ϵ_f	−0.9	−0.9	−1.6	−1.6
U_{fc}	11.2	11.2	10.7	10.7
U	6.8	6.8	7.0	7.0
FWHM	1.3	1.3	1.5	1.5
ϵ_c	21.3	3.2	21.15	3.1

would also be a f^4 peak 5.3 eV above the f^3 peak, which even has the biggest intensity.

IV. CONCLUSIONS

We have calculated appearance-potential spectra for $CePd_3$ and $CeNi_5$ in the framework of the Anderson-impurity model using the Gunnarsson-Schönhammer approach. The theoretical results are in good agreement with experimental data. We found that the procedure is as reliable in describing two-particle spectra as it was in the case of one-particle spectra. The main physics of the APS intensities in heavy-fermion systems is described by the strong correlation both between the fermions and between the $4f$ electrons and the core hole. In $4f$ systems, the self-convolution of one-particle spectra leads to unphysical results.

ACKNOWLEDGMENTS

We would like to thank O. Gunnarsson, K. Schönhammer, and K. Ertl for many useful discussions.

[1] V. Dose and H. Scheidt, Appl. Phys. **19**, 19 (1979).
[2] K. Ertl, M. Vonbank, V. Dose, and J. Noffke, Solid State Commun. **88**, 557 (1993).
[3] T. Detzel, Ph.D. thesis, Universität Bayreuth, 1994.
[4] J. J. Lander, Phys. Rev. **91**, 1382 (1953).
[5] M. Cini, Solid State Commun. **20**, 605 (1976).
[6] G. A. Sawatzky, Phys. Rev. Lett. **39**, 504 (1977).
[7] W. Nolting, Z. Phys. B **80**, 73 (1990).
[8] W. Nolting, G. Geipel, and K. Ertl, Phys. Rev. B **44**, 12 197 (1991).
[9] M. Potthoff, J. Braun, W. Nolting, and G. Borstel, Surf. Sci. **307-309**, 942 (1994).
[10] O. Gunnarsson and K. Schönhammer, in *Handbook on the Physics and Chemistry of Rare Earths*, edited by K. A. Gschneidner *et al.* (Elsevier Science, Amsterdam, 1987), p. 103.
[11] O. Gunnarsson and K. Schönhammer, Phys. Rev. B **28**, 4315 (1983).
[12] A. Kotani and Y. Toyozawa, J. Phys. Soc. Jpn. **37**, 563 (1974).
[13] A. Kotani and Y. Toyozawa, J. Phys. Soc. Jpn. **37**, 912 (1974).
[14] O. Gunnarsson and K. Schönhammer, Phys. Rev. Lett. **50**, 604 (1983).
[15] F. U. Hillebrecht, Ph.D. thesis, Kernforschunganlage Jülich, 1984.
[16] O. Gunnarsson and K. Schönhammer, Phys. Rev. B **22**, 3710 (1980).
[17] V. Dose, R. Drube, and A. Härtl, Solid State Commun. **57**, 273 (1986).
[18] T. V. Ranakrishnan, in *Valence Fluctuations in Solids*, edited by L. M. Falicov *et al.* (North-Holland, Amsterdam, 1982), p. 13.
[19] P. W. Anderson, *Valence Fluctuations in Solids* (Ref. 18), p. 451.
[20] J. A. Matthew, G. Strasser, and F. P. Netzer, Phys. Rev. B **27**, 5839 (1983).

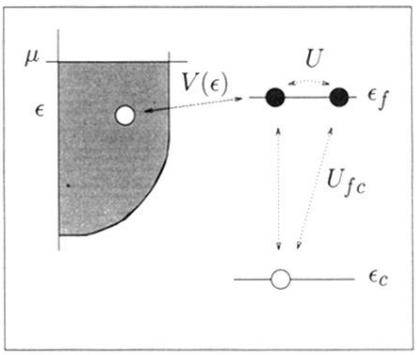

FIG. 1. Sketch of the physical processes covered by the AIM. The conduction band is filled up to chemical potential μ. Electrons in the f level at energy ϵ_f are scattered by the local Coulomb repulsion U, the core hole interaction U_{fc}, and the hybridization $V(\epsilon)$. The energy of the core level is ϵ_c.